ISA Transactions 138 (2023) 735–745

Contents lists available at ScienceDirect

ISA Transactions

journal homepage: www.elsevier.com/locate/isatrans

Practice article

Time and energy optimal trajectory generation for coverage motion in industrial machines

Mathias Sebastian Halinga [a,b,*], Enock William Nshama [b], Tobias Rainer Schäfle [c], Naoki Uchiyama [a]

[a] Department of Mechanical Engineering, Toyohashi University of Technology, Toyohashi, 441-8580, Japan
[b] Department of Mechanical and Industrial Engineering, University of Dar es Salaam, Dar es Salaam, 35091, Tanzania
[c] Fraunhofer Institute for Manufacturing Engineering and Automation IPA, Stuttgart, 70569, Germany

ARTICLE INFO

Article history:
Received 18 March 2022
Received in revised form 27 February 2023
Accepted 18 March 2023
Available online 20 March 2023

Keywords:
Computer numerical control machines
Feed drive systems
Multi-objective optimization
Pareto front
Path optimization
Trajectory generation

ABSTRACT

The increase in computer numerical control machine efficiency highly contributes to environmental emission reduction and energy-savings. Path and trajectory optimizations are used to improve machine efficiency in a coverage motion such as pocket milling, polishing, inspection, gluing, and additive manufacturing. Several studies have proposed coverage motion optimization in improving machine efficiency for time and energy consumption. Ensuring the smoothness and satisfaction of the machine constraints in coverage motion is necessary. This paper proposes a multi-objective path and trajectory optimization to obtain a trade-off between time and energy consumption for coverage motion. Jerk limited acceleration profiles describe the trajectory where velocity profiles generated for each linear segment attain desirable velocities. The energy model of an industrial two-axis feed drive system is used in finding solutions to the optimization problem. The non-dominated sorting genetic algorithm II generates a Pareto front for trade-off time and energy consumption solutions. Simulation results of the proposed method are validated through experiments using the industrial two-axis feed drive system. Experimental results show the effectiveness of the proposed approach where time reduction and energy savings are 10.05% and 2.10%, respectively. In addition, the optimized path has a lower maximum error of 76.6% compared to the constantly commanded velocity optimized path.

1. Introduction

Energy depletion and greenhouse emissions are global challenges that emphasize the need to improve manufacturing industry efficiency through energy savings. This industry is one of the sectors with high energy consumption [1]. Computer numerical control (CNC) machines used in the manufacturing industry consume energy and emit greenhouse gases during the running process [2–5]. Energy consumption during the material removal process accounts for 15%–20% of the total energy consumption of the machine [6]. Although CNC machines are widely used in manufacturing, numerous studies indicate that their efficiency is about 30% [7,8]. Hence, efficiency improvement is needed since such machines operate for a long time with repetitive tasks.

In CNC milling, several studies have been conducted on improving the time and energy efficiencies of the milling process. F. Han et al. propose the optimization model to obtain optimal parameters for power reduction in the milling process [9]. A multi-objective model for the milling process is proposed to maximize the energy efficiency and minimize the production time [10]. Nshama et al. [11] propose an energy consumption model for the two-axis feed drive system. The studies mentioned above present models for improving machine efficiency. Nevertheless, path optimization and trajectory generation should be considered to ensure smooth motion and further energy reduction. Moreover, machine efficiency improvement can be achieved through feedrate optimization/scheduling with trajectory generation. A feedrate optimization approach is proposed by Endo et al. for accurate prediction of cycle time for CNC machine path [12]. Feedrate optimization with higher-order constraints is presented using a heuristic trajectory generation algorithm for curved and linear toolpath to attain time-optimality satisfying machine tool drive constraints [13]. Sun et al. propose feedrate optimization for the five-axis machine; the optimal feedrates are obtained from the velocity, acceleration, and jerk limit to ensure the required machining accuracy while satisfying the machine kinematic limits [14]. Uchiyama et al. propose trajectory generation for a point-to-point motion for energy reduction and smooth motion generation [15]. Bossetti and Bertolazzi propose that the optimal and improved control motion can be attained

* Corresponding author at: Department of Mechanical Engineering, Toyohashi University of Technology, Toyohashi, 441-8580, Japan.
E-mail address: mathias.sebastian.halinga.cn@tut.jp (M.S. Halinga).

https://doi.org/10.1016/j.isatra.2023.03.025
0019-0578/

through accurate dynamic modeling and generating the trajectories with continuity [16]. A minimum-time trajectory generation using jerk-limited feedrates of a given point-to-point motion CNC toolpath is proposed [17]. Cycle time and motion accuracy trajectory generation for the two-axis feed drive system is proposed [18]. In [19], time-optimal trajectory generation is presented with consideration to kinematic and dynamic constraints for robotic manipulator along fully specified paths. Shen et al. [20] propose a time-optimal motion for ensuring the continuity of the acceleration trajectory for the robotic system path-constrained while operating with its constant optimal trajectory values. A minimum-energy trajectory generation on robotic systems is proposed for point-to-point motion using trapezoidal and cycloidal speed profiles [21]. Zhou et al. propose minimum-energy trajectory planning for robotic system of sculptured surface machining [22]. These studies show the necessity of trajectory generation/optimization in the coverage motion to improve machine efficiency in energy savings, cycle time, and motion smoothness. Generally, the time and energy consumed by industrial machines are affected not only by trajectory but also by the path. To further reduce time and energy consumption, optimal path selection is crucial [23,24]. However, the previous studies mentioned above, trajectory generation is implemented along the predefined contour paths.

In addition, the geometric path has an impact on machine efficiency; path optimization is another approach used in improving machine efficiency. Zhou et al. propose a toolpath optimization method in milling [25]. An improved genetic algorithm (GA) is used to generate and optimize the toolpath for cavity milling with simultaneous optimization of cutting parameters and the toolpath aiming to attain the best trade-off toolpath between processing time, cost, and energy. In [26], a toolpath optimization method for the free-form surface milling is proposed. An image process method on path optimization is proposed in [27]. The method improves the efficiency in pocket milling using a contour milling strategy. Hatem et al. propose an algorithm for geometric path optimization for CNC milling to achieve the shortest path [28]. Kumar and Khatak propose toolpath optimization through a discretization framework [29]. GA is used in toolpath optimization to minimize machining time and jerk for the machine efficiency improvement. In [30], toolpath optimization to minimize machining time on several linear segments in the area to be machined is proposed, in which GA and particle swarm algorithm (PSA) are used for optimization. Edem and Mativenga propose a feed-axes energy model to estimate time and power consumption for the CNC toolpath. The model is used to analyze the impacts of toolpath selection and geometry [31]. However, these studies present path optimization methods; trajectory generation, including velocity, acceleration, and jerk, is not considered. As a result, the optimized geometric path motion can generate high operating speeds, excessive accelerations, and vibrations of the machine's mechanical structure, which affect accuracy and performance. In addition, the same constant velocity command approach is used in [25,26] for geometric path optimization. For several linear segments of coverage motion, the commanded constant velocity may not be achieved by shorter segments leading to higher machine excitation. Therefore, it is of great importance to consider trajectory generation in path optimization to improve motion accuracy and efficiency.

In recent studies, GA proved to be effective in path optimization for improving machine efficiency. Zhou et al. use improved GA for toolpath optimization in cavity milling [25]. GA is used for toolpath optimization for free-form surface in [26]. GA is used for finding the optimal machining sequence in different areas for a blank flat workpiece in [29]. Pezer uses GA to attain the drilling sequence [32]. Although simple GA is used in multi-objective functions, objectives are combined into a single objective which may lead to the possibility of the search direction being in one point and diversity of solution being degraded [33,34]. Non-dominated sorting genetic algorithm II (NSGA II) is an efficient evolution algorithm used to provide a set of the Pareto optimal solutions by the Pareto dominance approach without combining objectives into a single objective function [35]. The algorithm maintains the diversity and elitism of the solutions using density estimation, crowding distance operator, and combining parents and offspring to generate the set of Pareto optimal solutions [36]. NSGA II is used to generate a non-dominating set of solutions for machine time, deviation, and energy consumption for feature sequencing [37]. Xue uses NSGA II for robot path planning to achieves shorter path, safety, and smoothness [38]. Beirigo et al. use NSGA II generates Pareto solutions set for time and cost in travel planning [39].

This study proposes a path and trajectory optimization method for time and energy optimal coverage motion which has wide applications such as pocket milling, inspection, polishing, gluing, and additive manufacturing. An energy model of a feed drive system is used to calculate the energy consumption for moving along the path with linear segments. Grids are generated to represent the point locations as path references. Jerk limited acceleration profile (JLAP) is used to describe the coverage motion with variable velocities depending on the length of the linear segment with full utilization of the machine performance. NSGA II is used to find the trade-offs between the two conflicting objectives: time and energy consumption. The Pareto front is generated to represent the trade-off between time and energy in a geometric path. The best trade-off solution is chosen as the optimal point nearest to the origin of the normalized objective function space. Experimental verification is carried out with a two-axis industrial machine. The smooth path motion is generated and compared to the case that constant velocity commands are used in path optimization [25]. The proposed approach achieves the best trade-off solution with the time reduction and energy-savings of approximately 10.05% and 2.10%, respectively. Also, the maximum error reduction is 76.6% compared to the constantly commanded velocity approach.

Following the discussion above, this study has two main contributions. The first is simultaneous trajectory generation and path optimization for the machine coverage motion. In most cases, two methods are implemented separately: trajectory generation [12–22] and path optimization [25–30]. Consideration of machine kinematic limits and geometric path simultaneously improves the accuracy, performance, and energy consumption of the industrial machine. Moreover, the proposed method has advantages for each linear segment to attain the desired velocity to ensure motion smoothness compared to the widely used approach of constant velocity command in path optimization [25,26]. The second contribution is the optimization of time and energy to generate the best trade-off solution. Optimization addresses the gap in the literature for time and energy consumption. Most similar studies that implement trajectory generation consider a single objective [12–17,19–22]. Because time and energy are two conflicting objectives, multi-objective optimization of time and energy is critical.

This paper is organized as follows: A description of trajectory representation is described in Section 2. Objective functions are given in Section 3, followed by the optimization algorithm in Section 4. Section 5 presents the optimization results. Section 6 discusses the experimental process and results, followed by concluding remarks in Section 7.

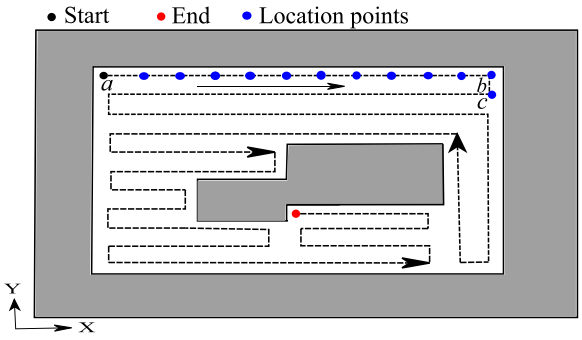

Fig. 1. Illustration of a path geometry.

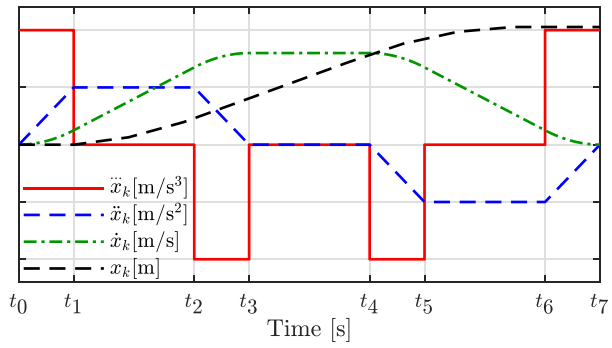

Fig. 2. Illustration of jerk limited acceleration profiles.

2. Trajectory representation

2.1. Path geometry

The path geometry is a series of location points for the coverage motion. For example in pocket milling, tool motion from one location point to another creates a linear segment. As shown in Fig. 1, motion from ***a*** to ***b*** passes through several location points to create a linear segment with motion distance L. The path consists of several linear segments. Motion ***a*** to ***b*** is the first segment and ***b*** to ***c*** is the second segment up to the end of the path. The connection of linear segments defines the generated geometric path.

For a given working surface whereby no information of the geometric path is given, the geometric path needs to be determined. To complete the coverage motion on the working surface from the start to the end of the motion, there are several different feasible paths. It is important to find the optimal geometric path based on objectives set for the coverage motion while satisfying the surface working constraints including obstacle avoidance (island) in this study. However, trajectory and machine kinematic limits such as velocity, acceleration, and jerk are not considered during geometric path optimization.

In linear motion interpolation, variables such as position, velocity, and acceleration are commanded to direct the motion from one location point to another while satisfying machine kinematic limits. Interpolation of these variables generates a trajectory or motion profile for each linear segment depending on the direction of axes. Trajectory generation for the linear segments needs to be performed for the machine to follow. The machine kinematic limits velocity, acceleration, and jerk should be observed to achieve the smooth coverage motion. Therefore, to increase the efficiency of the industrial machine, the objective functions of time and energy consumption are considered for the coverage motion with simultaneous geometric path optimization and trajectory generation.

2.2. Trajectory representation of linear segment

It is crucial to ensure smooth kinematic profiles during trajectory generation to maintain accuracy and avoid exciting the machine [40,41]. JLAP is used to generate smooth trajectories for accurate linear contours in path optimization. It is the trajectory with continuous acceleration profiles generated from seven segments motion time intervals, as shown in Fig. 2. The definition of the jerk in each time interval is

$$\dddot{x}_k(t) = \begin{cases} j_{\text{lim},k}, & t_0 \le t < t_1, \\ 0, & t_1 \le t < t_2, \\ -j_{\text{lim},k}, & t_2 \le t < t_3, \\ 0, & t_3 \le t < t_4, \\ -j_{\text{lim},k}, & t_4 \le t < t_5, \\ 0, & t_5 \le t < t_6, \\ j_{\text{lim},k}, & t_6 \le t < t_7. \end{cases} \tag{1}$$

The time intervals are determined by velocity, acceleration, and jerk limit, with the assumption that acceleration and deceleration are the same as the behavior of industrial machines. The definition of the time intervals are

$$\begin{aligned} t_{\text{a},1} &= t_1 - t_0 = t_3 - t_2 = t_5 - t_4 = t_7 - t_6, \\ t_{\text{c},1} &= t_2 - t_1 = t_6 - t_5, \\ T_{\text{c},1} &= t_4 - t_3, \end{aligned} \tag{2}$$

where j_{lim} is the jerk limit for the kth axis, $t_{\text{a},1}$ is the linear acceleration/deceleration period, $t_{\text{c},1}$ is the constant acceleration/deceleration period, and $T_{\text{c},1}$ is the constant velocity period.

For a linear segment distance L of the geometric path, all machine kinematic limits should be satisfied to determine the feasible and optimal coverage motions. The kinematic limits jerk, acceleration, and velocity must be $j_{\text{lim}}, a_{\text{lim}}, v_{\text{lim}} > 0$, and satisfy the following requirements:

$$\begin{aligned} |\dddot{x}_k(t)| &\le j_{\text{lim},k}, \\ |\ddot{x}_k(t)| &\le a_{\text{lim},k}, \\ |\dot{x}_k(t)| &\le v_{\text{lim},k}, \end{aligned} \tag{3}$$

where $x_k(t)$ is the displacement of axis k. $j_{\text{lim},k}$, $a_{\text{lim},k}$, and $v_{\text{lim},k}$ are the jerk, acceleration, and velocity limits, respectively. In this study, point-to-point linear contours are used with zero velocity, acceleration, and jerk at the start and final position of the linear segment.

3. Objective functions

3.1. Motion time

Motion time is the total time needed in moving the machine table to complete the motion along the path. During motion, the time for each linear segment, as suggested in [15], is calculated using (4). The total motion time is a summation of all segment times of the path. The time for each linear segment is calculated as

$$T_i = T_{\text{c},i} + 2t_{\text{c},i} + 4t_{\text{a},i}, \tag{4}$$

where T_i is the required time for motion distance of the ith segment, $T_{\text{c},i}$ is the constant velocity period of the ith segment,

Table 1
Energy coefficients of each drive axis.

$k$thaxis		$c_{1,k}$ [W s^4/m^2]	$c_{2,k}$ [W s^2/m^2]	$c_{3,k}$ [W s/m]	$c_{4,k}$ [W]	$c_{5,k}$ [W s^2/m]	$c_{6,k}$ [W s^3/m^2]
x	$\dot{x} \geq 0$	2.684	546.357	45.135	0.663	2.2667	90.838
	$\dot{x} < 0$	2.684	476.807	−52.333	0.891	−3.093	90.838
y	$\dot{y} \geq 0$	2.101	534.437	50.851	0.856	2.682	79.682
	$\dot{y} < 0$	2.101	494.006	−48.999	0.795	−2.584	79.682

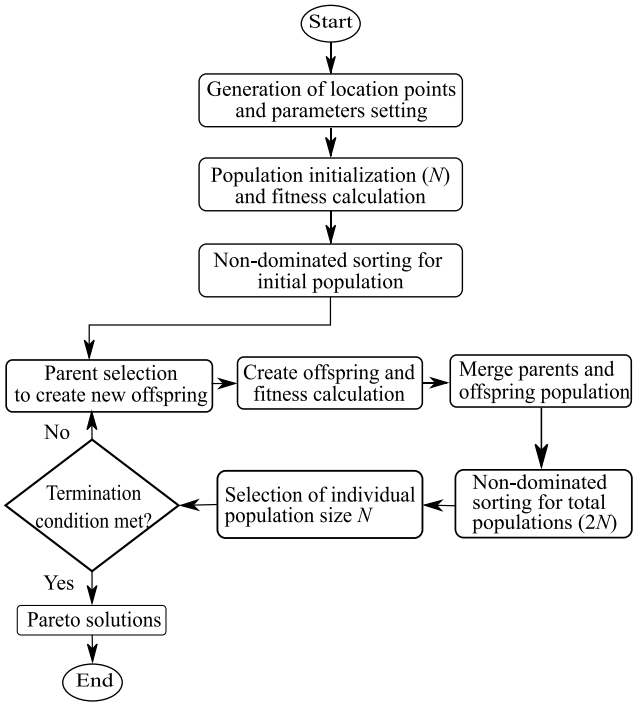

Fig. 3. Illustration of a flow chart for NSGA II.

$t_{c,i}$ is the constant acceleration/deceleration period of the ith segment, and $t_{a,i}$ is the linear acceleration/deceleration period of the ith segment.

3.2. Energy consumption

For linear segment trajectory, position, velocity, and acceleration determine the energy consumption for industrial feed drive systems [15]. Hence, it is essential to incorporate these factors in path optimization. The energy consumption model used in this study is from [11], which incorporates dynamics of feed drive systems. The energy model is formulated using a two-axis industrial feed drive system with AC 3ϕ motors. As proposed in [15], the output power P is given by

$$P = \sqrt{3}\lambda V(t) I(t), \tag{5}$$

where $V(t)$ and $I(t)$ are the instantaneous effective voltage and current of a motor, respectively. λ is the power factor for each axis and it is assumed to be constant when the load range of the motor is greater than a certain value. The effective voltage and current are given by

$$V(t) = I(t)Z + K_E\dot{x}(t), \tag{6}$$

with

$$Z = \text{diag}\{z_k\},\ K_E = \text{diag}\{k_{E,k}\},$$

$$I(t) = \frac{1}{K_F}[M\ddot{x}(t) + D\dot{x}(t) + F\text{sgn}\{\dot{x}(t)\}], \tag{7}$$

Table 2
Parameters values of each drive axis.

$k$thaxis	m_k [N s^2/m]	d_k [N s/m]	f_k[N]	$k_{F,k}$ [N/A]
x	86.76	558.62	47.50	235.62
y	99.65	795.5	58.00	331.12

with

$$M = \text{diag}\{m_k\}, D = \text{diag}\{d_k\}, F = \text{diag}\{f_k\},$$
$$K_F = \text{diag}\{k_{F,k}\}, k \in \{x, y\},$$

where z_k is the motor impedance, $k_{E,k}$ is the back EMF coefficient, m_k is the inertia of the drives, d_k is the viscous friction, f_k is the Coulomb friction, and $k_{F,k}$ is the constant force.

The combination of (5)–(7) leads to an electric power consumption given by

$$P_k = C_{1,k}\ddot{x}_k^2 + C_{2,k}\dot{x}_k^2 + C_{3,k}\dot{x}_k\text{sgn}(\dot{x}_k) + C_{4,k}$$
$$+C_{5,k}\ddot{x}_k\text{sgn}(\dot{x}_k) + C_{6,k}\ddot{x}_k\dot{x}_k, \quad \text{for} \quad k = \{x, y\},$$

with

$$C_j = \text{diag}\{c_j, k\},\ j = \{1, 2, \ldots., 6\},$$
$$c_{1,k} = \sqrt{3}\lambda_k m_k^2 \frac{z_k}{k_{F,k}^2},$$
$$c_{2,k} = \sqrt{3}\lambda_k d_k \left(\frac{z_k d_k}{k_{F,k}^2} + \frac{k_{E,k}}{k_{F,k}}\right),$$
$$c_{3,k} = \sqrt{3}\lambda_k f_k \left(\frac{2z_k d_k}{k_{F,k}^2} + \frac{k_{E,k}}{k_{F,k}}\right),$$
$$c_{4,k} = \sqrt{3}\lambda_k f_k^2 \frac{z_k}{k_{F,k}^2},$$
$$c_{5,k} = 2\sqrt{3}\lambda_k f_k m_k \frac{z_k}{k_{F,k}^2},$$
$$c_{6,k} = \sqrt{3}\lambda_k m_k \left(\frac{2z_k d_k}{k_{F,k}^2} + \frac{k_{E,k}}{k_{F,k}}\right), \tag{8}$$

where $c_{j,k}$ is the jth coefficient for the kth axis.

The important property is that power is a function of velocity and acceleration. Therefore, the power can be estimated from trajectory profiles. Energy is calculated for each linear segment. The summation of energy for all segments gives the total energy of the coverage motion. Energy consumption for the linear segment is given by

$$E = \int_{t_0}^{t_{tf}} (|P_x(t)| + |P_y(t)|)dt, \tag{9}$$

where E is the total energy consumption for the feed drive system, t_0 and t_{tf} are the start and end motion time of the segment, respectively. $P_x(t)$ and $P_y(t)$ are the power at time t for the x and y axis, respectively.

Different machine coefficients and parameters used in this study are presented in Tables 1 and 2, respectively.

3.3. Multi-objective model

The multi-objective model is used to obtain the trade-off between time and consumed energy in minimizing both objectives.

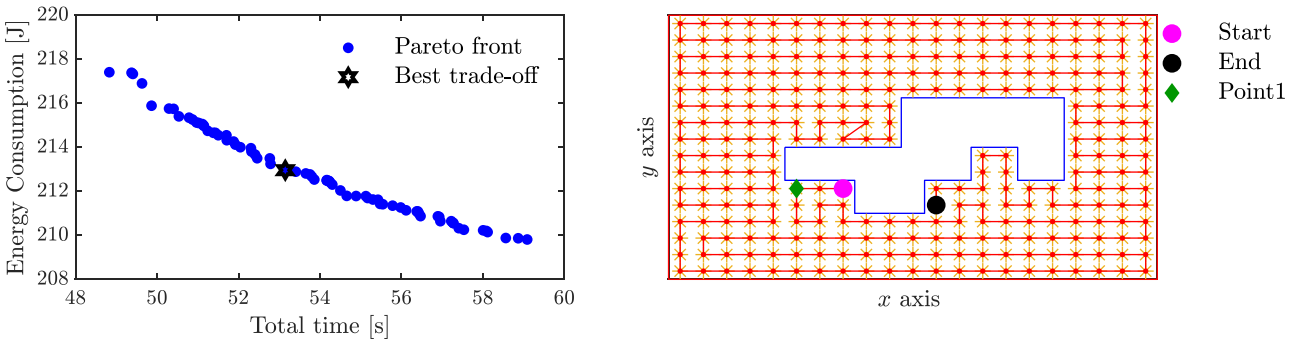

(a) Pareto front (b) Best trade-off path

Fig. 4. Pareto front representing the optimization results and the geometric path at the best trade-off.

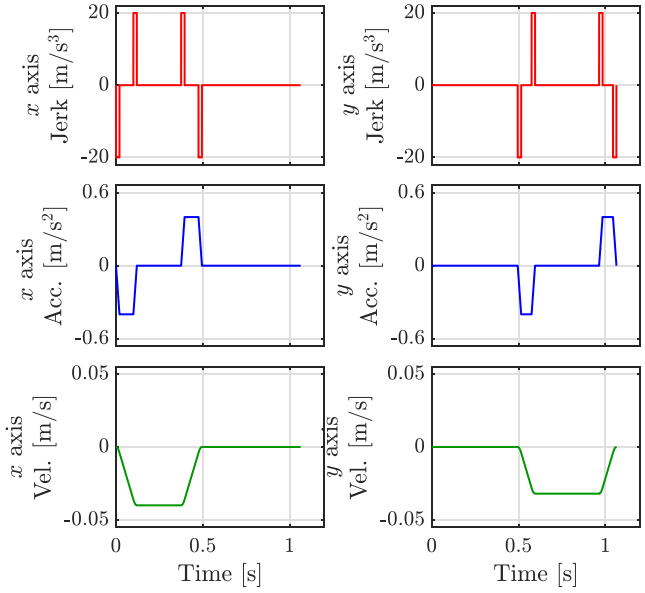

Fig. 5. The best trade-off path's generated jerk, acceleration, and velocity for a linear segments in x and y axes.

The representation of the model is expressed as

$$F(\mathbf{z}) = \min_{\mathbf{z}}\{T(\mathbf{z}), E(\mathbf{z})\}, \tag{10}$$

where T and E are the time and energy consumption for the entire coverage motion, respectively, and $\mathbf{z}$ is an optimization parameter vector that consists of variables describing the coverage motion. The optimization parameters are the time intervals and linear segment distance described as

$$\mathbf{z} = [t_{a,1}, t_{c,1}, T_{c,1}, L]. \tag{11}$$

4. Optimization of the model using NSGA II

NSGA II starts with initial solutions and then gets modified through the iteration process using different operators. Fig. 3 shows an optimization flow process. Each operation is described as follows.

4.1. Location points generation

For the machine table to move from one point to another on the working surface, the series connection of the points defines the path. A series of location points is necessary for path generation to achieve the desired geometric path. After specifying the working surface, point locations are generated on it with equal distance from one point to another, which is 7.5 mm in this study. Grid points represent location points and are stored using x and y coordinates. Numbering is assigned for each grid location point.

4.2. Encoding

Numbers are used to generate different solutions representing different coverage paths. With no repetition, each number/integer represents a location point, in a sequence such as $1 \rightarrow 4 \rightarrow 6 \rightarrow 2 \rightarrow 7 \rightarrow 3 \rightarrow 5$, where the motion starts at 1 followed by 4 up to 5. In NSGA II, each number is a gene with point information; all genes for the path create chromosomes called population. The total number of genes in the path equals the number of series location points representing the geometric path.

4.3. Population initialization

The initial population is a set of chromosomes representing different options for the coverage motion. Initialization is a critical step to obtain the best results. If the total population is randomly initialized, an optimal solution is obtained after a long time [42]. Two methods are used for population initialization: random and heuristic. In this study, 80% of the population is randomly generated to maintain diversity and optimality in solutions, and the remaining population is heuristically initialized.

4.4. Fitness functions

Fitness functions are used to obtain solution values at each algorithm run. The fitness functions are expressed as

$$T = \sum_{i=1}^{n}\left(T_{c,i} + 2t_{c,i} + 4t_{a,i}\right), \tag{12}$$

$$E = \int_{t_0}^{t_{tf}} |P_k(t)|dt, \tag{13}$$

where T is the total time, E is the total energy, $T_{c,i}$ is the constant velocity period of the ith segment, $t_{c,i}$ is the constant acceleration/deceleration period of the ith segment, and $t_{a,i}$ is the linear acceleration/deceleration period of the ith segment. $P_k(t)$ is the power at time t for the kth axis, t_0 is the start motion time, and t_{tf} is the end motion time.

4.5. Selection

Parents are individuals, as analogous to reproduction, used to create offspring in the recombination process. Individuals in the population of size N are selected to be parents. In this study, binary tournament selection is used, as proposed in [36], based on crowding distance comparison.

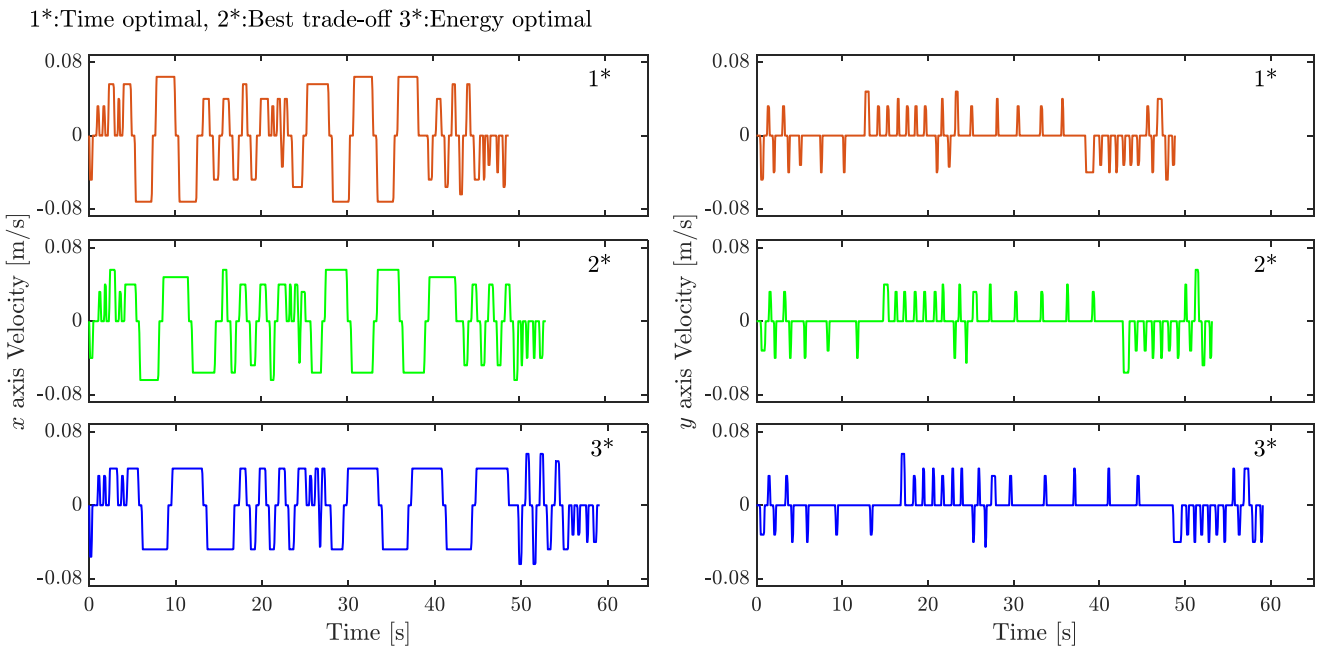

Fig. 6. Generated velocity profiles for the time, best trade-off, and energy optimality paths in x and y axes.

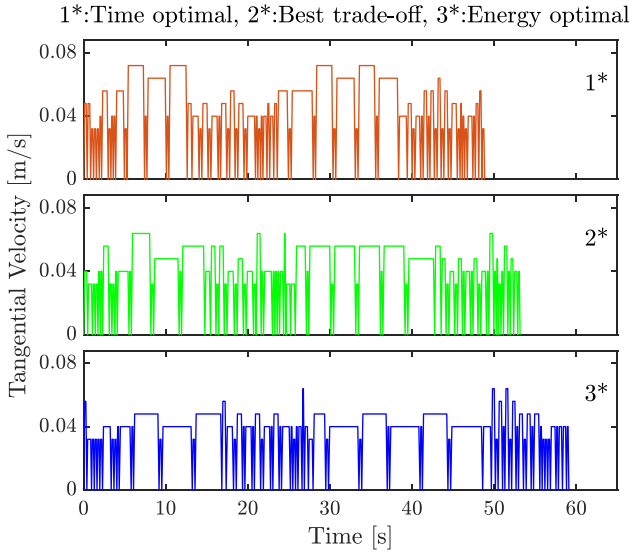

Fig. 7. Generated tangential velocities for the time, best trade-off, and energy optimality paths.

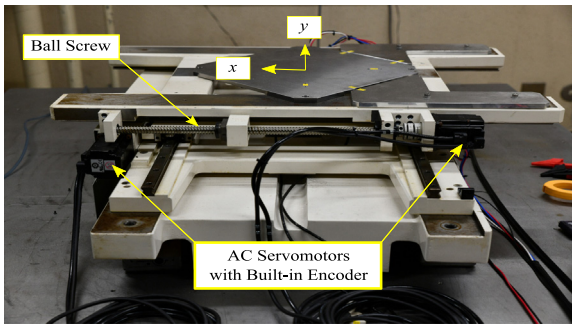

Fig. 8. Two-axis industrial machine.

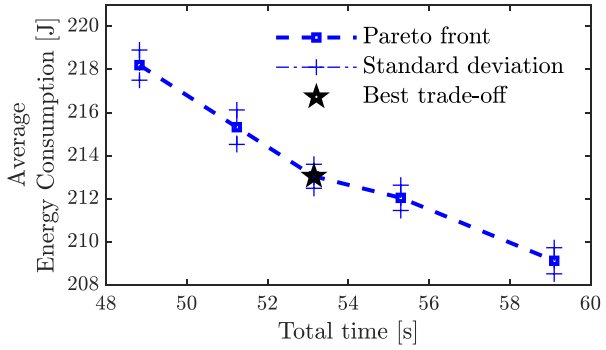

Fig. 9. Experimental results on energy consumption.

4.6. Crossover operation

The crossover is a recombination process that creates offspring from a pair of parents that exchange their genes, creating two offspring. The crossover probability *pc* is set to the algorithm as a crossover occurrence in the population. Table 3 illustrates the order crossover operation, where a pair of parents is selected, and two random cuts divide parents into three separate groups of genes. For creating the first offspring, the genes between the two cuts in the second parent are copied to fill the position in the offspring while maintaining their position, and the remaining genes are filled by first parent genes not occupied in the offspring. The second offspring is created copying genes in between the two cuts of the first parent by maintaining their position as in the parent. The remaining part is filled by the genes found in the second parent but not found in the second offspring.

4.7. Mutation operation

Mutation operation improves newly formed offspring during the iteration process after the crossover operation by making small changes to the selected genes. In this study, inversion mutation is used in combination with a local search to improve the solutions. Table 4 shows the mutation process. In inversion

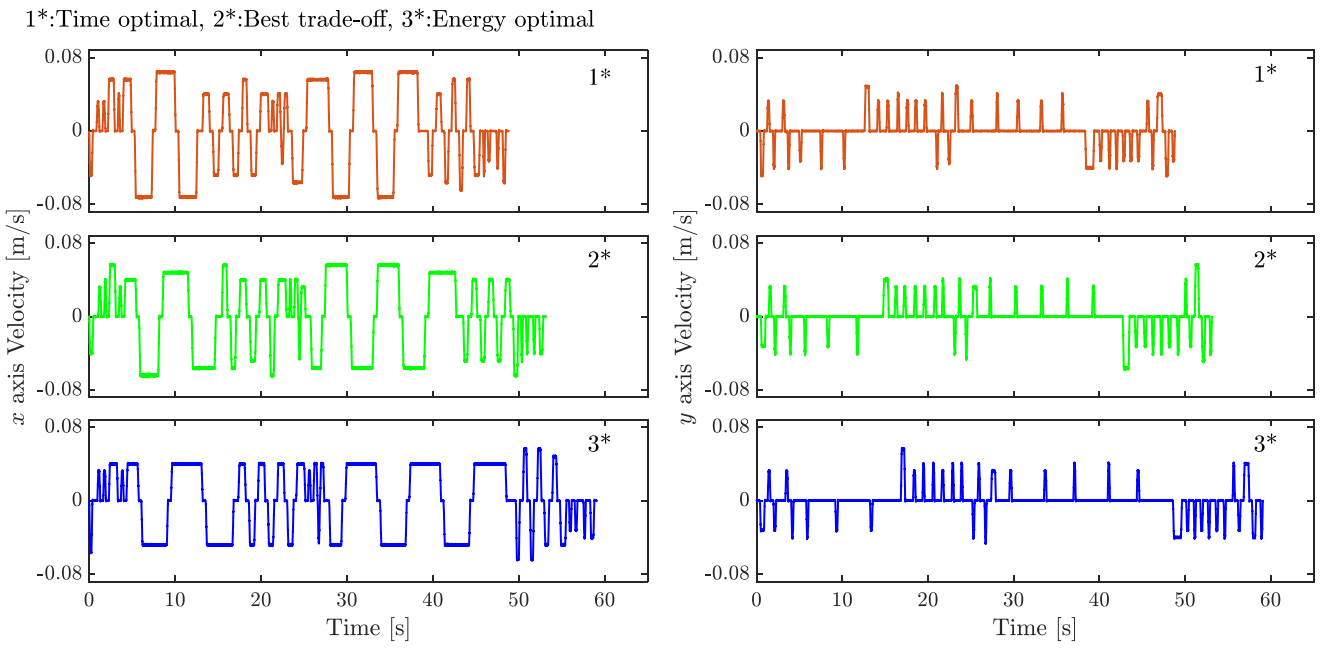

Fig. 10. Experimental velocity profiles for the time, best trade-off, and energy optimality paths in x and y axes.

Table 3
Crossover process.

Chromosome	Genes
parent (1)	$1 \to 4 \to \underbrace{6 \to 2 \to 7} \to 3 \to 5$
parent (2)	$2 \to 5 \to \underbrace{1 \to 4 \to 7} \to 6 \to 3$
offspring (1)	$6 \to 2 \to \underbrace{1 \to 4 \to 7} \to 3 \to 5$
offspring (2)	$5 \to 1 \to \underbrace{6 \to 2 \to 7} \to 4 \to 3$

Table 4
Mutation process.

Chromosome	Genes
parent	$1 \to 4 \to \underbrace{6 \to 2 \to 7 \to 3} \to 5$
offspring	$1 \to 4 \to \overbrace{3 \to 7 \to 2 \to 6} \to 5$

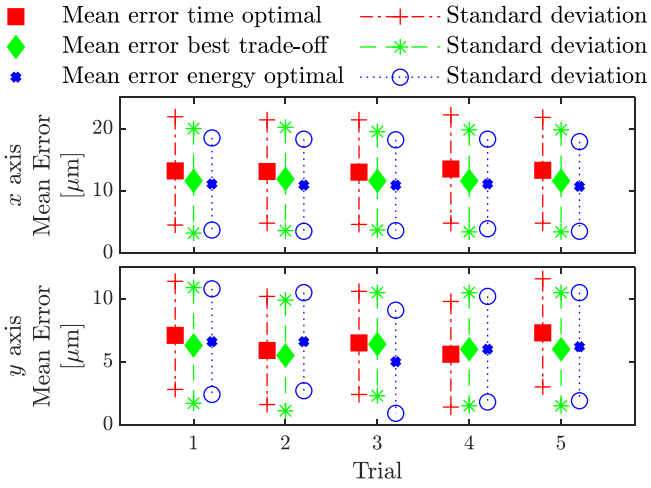

Fig. 11. Mean absolute tracking error for the time, best trade-off, and energy optimality paths in x and y axes.

mutation, uniformly random two cut points are generated, and the genes between the two cuts are inverted to form new offspring. The local search finds the best new mutated offspring during the inversion process compared to an initial individual; there is no improvement if the initial individual is better than the mutated offspring.

4.8. Merging and sorting

After the crossover and mutation process, the newly formed population offspring of size N combine with the initial population parents to form a new population of size $2N$. The formed population is sorted based on their dominance to generate Pareto fronts, starting with the first Pareto front to obtain population size N. The sorted population size N becomes the new population for the subsequent recombination of operation or the final Pareto solutions, as illustrated in Fig. 3.

4.9. Termination condition

The algorithm runs several iterations to improve solutions, and the maximum number of iterations is predefined. The number is selected based on trial runs by checking if the solutions have no further improvement of the fitness values.

4.10. Computation complexity

The computational burden is the amount of resources required to perform a computation. It is described in terms of time and space resources [43]. In running the optimization problem by NSGA II, the resource space complexity is described as $O(n_p^2)$, where n_p is the population size [44]. Time burden is given by $O(n_{it} n_o n_p^2)$, where n_{it}, n_o, and n_p are number of iterations, objectives, and population size, respectively [43,44]. Thus, the optimization problem in this study has a space and time complexity of $O(n_p^2)$ and $O(n_{it} n_o n_p^2)$, respectively.

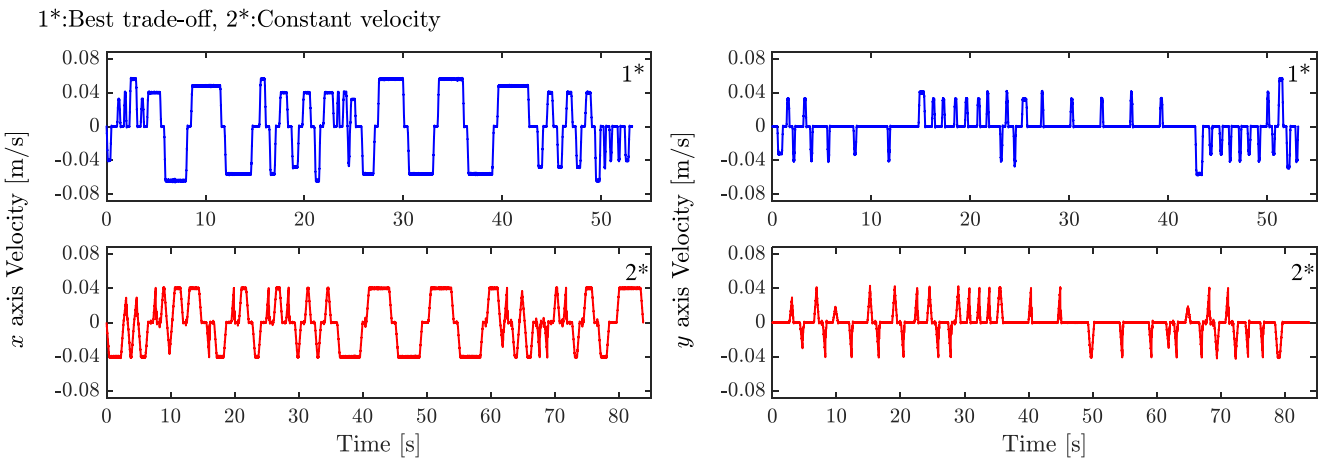

Fig. 12. Experimental velocity profiles for the best trade-off and constantly commanded velocity paths in x and y axes.

5. Case study

5.1. Optimization condition

The 2D pocket geometry part in Fig. 4(b) is used for path optimization. The working surface dimensions are 158.5 mm x 120 mm with a polygon as the island is used. The axial velocity, acceleration, and jerk machine limits are 0.08 m/s, 1 m/s^2, and 20 m/s^3, respectively. The optimization problems of (12) and (13) are used as fitness functions in NSGA II to determine optimal motion time and energy consumption along the geometric paths. NSGA II parameters are crossover probability $pc = 0.8$, mutation probability $pm = 0.2$, population size is 200, and maximum iterations number is 100. The parameters are selected based on trial runs of different parameters set of pc, pm, population size, and a maximum number of iterations by checking if the solutions have no further improvement of the fitness values. The optimization is performed in MATLAB 2021a environment on a laptop computer core i7-1165G7, 2.80 GHz CPU, 16 GB RAM, and Windows 10 operating system to generate optimized solutions.

5.2. Optimization results

The Pareto front is generated after running the algorithm for 100 iterations. Fig. 4(a) shows the Pareto front for the trade-off between total time and energy consumption, and Fig. 4(b) shows the best trade-off geometric path. At the best trade-off point in Fig. 4(a), the energy consumed is 212.96 J and the total time path motion is 53.15 s. At the energy-optimal point, the path motion energy consumption is 209.81 J and the total time is 59.09 s. The energy consumed is 3.15 J, less than the best trade-off path energy consumption. At the time-optimal point, the energy consumption is 217.52 J, which is 4.56 J higher than the best trade-off point, and the total time is 48.83 s. Hence, the best trade-off solution provides time reduction and energy savings of 10.05% and 2.10%, respectively, compared to the time and energy-optimal solutions. As shown in Fig. 4, the Pareto optimal results indicate that the proposed approach is effective in finding the trade-off between two objectives. The computation time for generating the Pareto optimal results (Fig. 4) is 754.98 s.

Path motion profiles for the jerk, acceleration, and velocity in optimal case of the best trade-off are presented in Fig. 5 for the x and y axes, a linear segment motion as shown in Fig. 4(b) from ***Start*** to ***Point1*** is used to generate the motion profiles. Velocity profiles for the time, best trade-off, and energy optimal solutions for both axes are shown in Fig. 6. The kinematic limits of all path motions are obeyed. Further, the proposed approach generates the path motion profiles with variable velocities for each linear segment. Tangential velocity is presented in Fig. 7. Trajectories are generated for each linear segment consisting of acceleration, constant velocity, and deceleration periods, which is a profile used in industrial machines to generate a smooth motion [15]. Furthermore, the optimized geometric path has longer segments that minimize the tool's frequent lifting and reduce air time; this contributes to significant time reduction and energy savings.

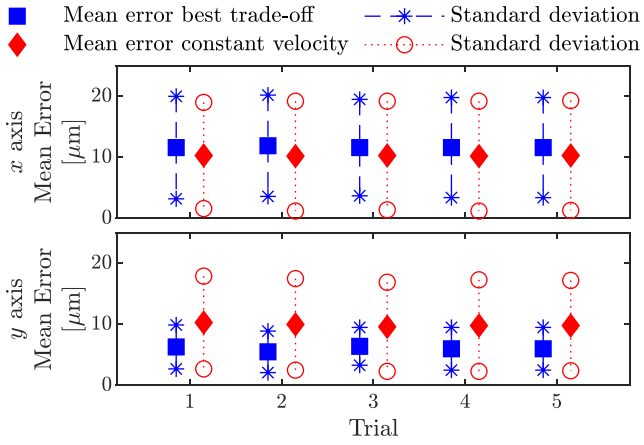

Fig. 13. Mean absolute tracking error for the best trade-off and constantly commanded velocity paths in x and y axes.

6. Experiment

6.1. Experimental procedure

An industrial two-axis machine, as shown in Fig. 8, is used in the experimental verification of the proposed approach. The machine table has two AC servomotors with two ball screw drive systems connected to each axis. The rotary encoders of 76.29 nm resolution are used to measure the axial position of each axis of the table. A sampling time of 0.2 ms is used.

The experiment is conducted on optimized paths from Pareto optimal solutions to verify the simulation results. Five points are selected on the Pareto front for experimental verification: best trade-off, energy-optimal, time-optimal solutions, and two other solutions, as shown in Table 5. Reference trajectories of the paths are prepared to move the machine, and the experiment of each path is repeated five times to ensure the repeatability of the results. The electrical power consumption for each axis is recorded

Table 5
Selected optimized paths on Pareto front.

No.	Total time [s]	Energy consumption [J]
1	48.83	217.52
2	51.24	214.75
3	53.15	212.96
4	55.30	211.63
5	59.09	209.81

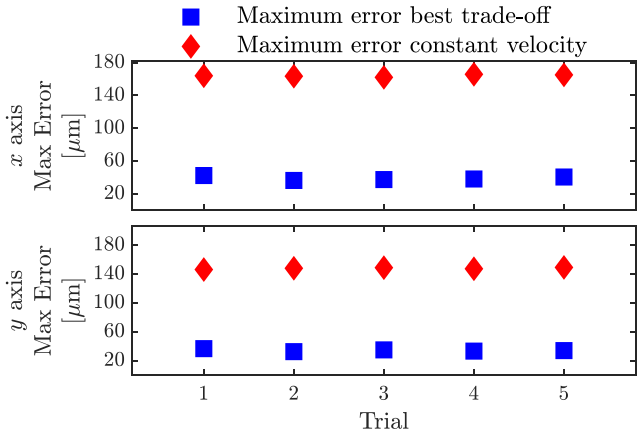

Fig. 14. Maximum error for the best trade-off and constantly commanded velocity paths in x and y axes.

by a power analyzer (HIOKI3390). The power analyzer is installed between a motor driver and a motor, directly measuring its power consumption. The analyzer measures energy using an integration measurement approach, in which the power is integrated every 50 ms of data update. When the reference trajectory path moves the machine, the measurement value of energy consumption for the two axes is displayed on the display channel. The total energy of the two axes is recorded. The experiment is repeated five times for each trajectory path, and the average energy consumption is calculated.

6.2. Experimental results

Experimental average energy consumption for five different paths selected from the Pareto front are presented in Fig. 9. The experimental results obtained are similar to the simulation results (see Fig. 4(a)). Experimental x and y axes velocity profiles for the time, best trade-off, and energy optimal cases are presented in Fig. 10. All the kinematic limits are obeyed and are similar to the velocity profiles for the simulation results (see Fig. 6).

The rotary encoder measures the tracking performance for the path motions. Fig. 11 shows the x and y axes mean absolute tracking error for the three paths: time, best trade-off, and energy optimal. The tracking error at the time-optimal path is higher in x axis when compared with other paths due to higher velocities attained by different linear segments in the path as shown in Fig. 10. The tracking error in y axes is similar in all of the paths since all short segments attain almost the same velocity.

Furthermore, the same constant velocity approach [25] is used for path and trajectory optimization to command all linear segments to achieve the commanded velocity. The selected velocity is 0.04 m/s. The generated path is compared with the optimized best trade-off path of the proposed approach. Fig. 12 shows the experimental velocity profiles for the best trade-off and constantly commanded velocity path for the x and y axes. The best trade-off path shows that each segment attains different desirable velocities. For the constantly commanded velocity approach, each linear segment tries to attain the desired constant velocity. However, short segments fail to attain it, leading to higher machine excitation and higher maximum errors than the proposed approach. Fig. 13 shows the mean absolute tracking error for the best trade-off and constantly commanded velocity approach. There is a slightly higher mean absolute tracking error for the best trade-off path in x axis compared to the constantly commanded velocity path because there are linear segments with higher assigned velocities, which is easier to be tracked by the controller. In the y axis, the constantly commanded velocity path has a higher mean absolute tracking error because almost all the segments have higher velocities compared to the best trade-off path.

Fig. 14 shows the maximum error for the two paths. Constantly commanded velocity path has a higher maximum error in both axes. The constant velocity cannot be attained for shorter linear segments, causing higher machine excitation. The best trade-off path has an approximately 76.6% reduced maximum error because all linear segments attain desirable velocities. The above results show that path optimization with variable velocities generates smoother motion profiles than the constantly commanded velocity approach. In addition, the energy consumption for the constant velocity path is 221.47 J, which is 3.8% higher than the best trade-off path.

6.3. Discussion

The study aims to solve the multi-objective problem of simultaneous path optimization and trajectory generation to minimize time and energy consumption for the coverage motion. As shown in Figs. 4(a) and 9 similar Pareto fronts are obtained in both simulation and experimental results. The optimal solution for the best trade-off between time and energy consumption is determined. The findings demonstrate that the proposed method can be used to provide a trade-off between time and energy consumption for the coverage motion (see Fig. 4(a) and 9). Hence, during process planning, the planner can choose any solution from the Pareto front, depending on the preferences between the two objectives.

Figs. 4(b) and 6 show simulation results of the generated geometric path and the motion profiles, respectively. From the simulation results, reference trajectories of the paths are prepared to move the machine table. The experimental motion profiles are recorded and plotted; the motion profiles are similar to simulated ones (see Figs. 6 and 10). From these results, we can conclude that the proposed method can achieve simultaneous path optimization and trajectory generation while obeying kinematic constraints. Unlike the path optimization in [25–30], which mainly generates an optimal geometric path without taking into account kinematic constraints, the proposed method generates the optimal path while considering trajectory generation, including velocity, acceleration, and jerk.

The proposed approach is compared with the same constant velocity approach used in path optimization [25]. The selected approach is widely used in practice for geometric path coverage motion optimization. To show the same performance, the mean absolute tracking and maximum error values are shown in Figs. 13 and 14. The proposed method shows a significant contribution in reducing the maximum error by 76.6%. As a result, it is reasonable to conclude that the proposed method can be used to improve motion performance.

In this study, the energy model of an industrial two-axis feed drive system (9) is used. Two-axis industrial machine feed drive systems are commonly utilized in the manufacturing industry, where they are found in types of machinery such as CNC milling, laser, and waterjet cutting machines. Therefore, the trajectory generation performance evaluation is performed on an industrial two-axis feed drive system. Since the trajectory evaluation is

done on a typical feed drive system, the proposed method can be applied to machining operations by simply incorporating a cutting force model. In addition, the proposed approach can be appropriate in pocket milling with the island since several linear segments have different lengths.

The limitation of the proposed approach is that the energy model does not yet incorporate the cutting force model and other related machining parameters. A cutting force model and other machine limitations, such as spindle speed, maximum cutting force, and surface roughness, should be included to enhance the machining performance. Our future work will take this into account.

7. Conclusion

This study proposes simultaneous path and trajectory optimization to minimize the time and energy consumption of the 2D coverage motion. An energy consumption model for a two-axis industrial machine is used in the optimization. Simulation results are verified using a two-axis industrial machine, which shows the effectiveness of the proposed approach. The best trade-off solution achieves a time reduction and energy savings of 10.05% and 2.10%, respectively. In addition, the proposed method improves the path's accuracy by reducing tracking errors. Results show that an optimized path motion with variable velocities at each linear segment lowers the maximum error by approximately 76.6% compared to the optimized path using the constant commanded velocity approach. Since machine efficiency improvement has several measures, multiple objectives can be added to find the Pareto optimal solutions.

Declaration of competing interest

The authors declare that they have no known competing financial interests or personal relationships that could have appeared to influence the work reported in this paper.

Acknowledgments

This work was supported in part by the Machine Tool Technologies Research Foundation, San Francisco, USA, Magnescale Company Ltd., Kanagawa, Japan, the Ministry of Education, Culture, Sports, Science and Technology, Japan, and JSPS, Japan KAKENHI under grant JP20KO4361.

References

[1] Menghi R, Papetti A, Germani M, Marconi M. Energy efficiency of manufacturing systems: A review of energy assessment methods and tools. J Clean Prod 2019;240:118276. http://dx.doi.org/10.1016/j.jclepro.2019.118276, URL https://www.sciencedirect.com/science/article/pii/S0959652619331464.

[2] Sihag N, Sangwan KS. A systematic literature review on machine tool energy consumption. J Clean Prod 2020;275:123125.

[3] Wan N, Zhuang Q, Chang Z, Yi Z. An allowance optimization method for near-net-shape blade considering material-saving, energy consumption and carbon emissions. Int J Environ Sci Technol 2022;1–16.

[4] Chen X, Li C, Tang Y, Li L, Li H. Energy efficient cutting parameter optimization. Front Mech Eng 2021;1–28.

[5] Cai W, Wang L, Li L, Xie J, Jia S, Zhang X, et al. A review on methods of energy performance improvement towards sustainable manufacturing from perspectives of energy monitoring, evaluation, optimization and benchmarking. Renew Sustain Energy Rev 2022;159:112227. http://dx.doi.org/10.1016/j.rser.2022.112227, URL https://www.sciencedirect.com/science/article/pii/S1364032122001502.

[6] Li L, Li C, Tang Y, Yi Q. Influence factors and operational strategies for energy efficiency improvement of CNC machining. J Clean Prod 2017;161:220–38. http://dx.doi.org/10.1016/j.jclepro.2017.05.084, URL https://www.sciencedirect.com/science/article/pii/S0959652617310168.

[7] Zhao J, Li L, Wang Y, Sutherland JW. Impact of surface machining complexity on energy consumption and efficiency in CNC milling. Int J Adv Manuf Technol 2019;102(9):2891–905.

[8] Cai W, Liu F, Zhou X, Xie J. Fine energy consumption allowance of workpieces in the mechanical manufacturing industry. Energy 2016;114:623–33. http://dx.doi.org/10.1016/j.energy.2016.08.028, URL https://www.sciencedirect.com/science/article/pii/S0360544216311318.

[9] Han F, Li L, Cai W, Li C, Deng X, Sutherland JW. Parameters optimization considering the trade-off between cutting power and MRR based on linear decreasing particle swarm algorithm in milling. J Clean Prod 2020;262:121388. http://dx.doi.org/10.1016/j.jclepro.2020.121388, URL https://www.sciencedirect.com/science/article/pii/S0959652620314359.

[10] Li C, Li L, Tang Y, Zhu Y, Li L. A comprehensive approach to parameters optimization of energy-aware CNC milling. J Intell Manuf 2019;30(1):123–38.

[11] Nshama EW, Msukwa MR, Uchiyama N. A trade-off between energy saving and cycle time reduction by Pareto optimal corner smoothing in industrial feed drive systems. IEEE Access 2021;9:23579–94.

[12] Endo M, Sencer B. Accurate prediction of machining cycle times by data-driven modelling of NC system's interpolation dynamics. CIRP Ann 2022. http://dx.doi.org/10.1016/j.cirp.2022.04.017, URL https://www.sciencedirect.com/science/article/pii/S0007850622000671.

[13] Erkorkmaz K, Layegh SE, Lazoglu I, Erdim H. Feedrate optimization for freeform milling considering constraints from the feed drive system and process mechanics. CIRP Ann 2013;62(1):395–8. http://dx.doi.org/10.1016/j.cirp.2013.03.084, URL https://www.sciencedirect.com/science/article/pii/S0007850613000851.

[14] Sun Y, Chen M, Jia J, Lee Y-S, Guo D. Jerk-limited feedrate scheduling and optimization for five-axis machining using new piecewise linear programming approach. Sci China Technol Sci 2019;62(7):1067–81.

[15] Uchiyama N, Goto K, Sano S. Analysis of energy consumption in fundamental motion of industrial machines and experimental verification. In: 2015 American control conference. IEEE; 2015, p. 2179–84.

[16] Bosetti P, Bertolazzi E. Feed-rate and trajectory optimization for CNC machine tools. Robot Comput-Integr Manuf 2014;30(6):667–77. http://dx.doi.org/10.1016/j.rcim.2014.03.009, URL https://www.sciencedirect.com/science/article/pii/S0736584514000258.

[17] Ward R, Sencer B, Jones B, Ozturk E. Accurate prediction of machining feedrate and cycle times considering interpolator dynamics. Int J Adv Manuf Technol 2021;116(1):417–38.

[18] Nshama EW, Uchiyama N. Pareto optimization of cycle time and motion accuracy in trajectory planning for industrial feed drive systems. IEEE Access 2021;9:114104–19.

[19] Barnett E, Gosselin C. A bisection algorithm for time-optimal trajectory planning along fully specified paths. IEEE Trans Robot 2020;37(1):131–45.

[20] Shen P, Zhang X, Fang Y, Yuan M. Real-time acceleration-continuous path-constrained trajectory planning with built-in tradeoff between cruise and time-optimal motions. IEEE Trans Autom Sci Eng 2020;17(4):1911–24.

[21] Carabin G, Scalera L. On the trajectory planning for energy efficiency in industrial robotic systems. Robotics 2020;9(4):89.

[22] Zhou J, Cao H, Jiang P, Li C, Yi H, Liu M. Energy-saving trajectory planning for robotic high-speed milling of sculptured surfaces. IEEE Trans Autom Sci Eng 2021.

[23] Feng C, Chen X, Zhang J, Huang Y, Qu Z. Minimizing the energy consumption of hole machining integrating the optimization of tool path and cutting parameters on CNC machines. Int J Adv Manuf Technol 2022;1–14.

[24] Edem I, Balogun V. Energy efficiency analyses of toolpaths in a pocket milling process. Int J Eng 2018;31(5):847–55.

[25] Zhou G, Zhang C, Lu F, Zhang J. Integrated optimization of cutting parameters and tool path for cavity milling considering carbon emissions. J Clean Prod 2020;250:119454. http://dx.doi.org/10.1016/j.jclepro.2019.119454, URL https://www.sciencedirect.com/science/article/pii/S0959652619343240.

[26] Li L, Deng X, Zhao J, Zhao F, Sutherland JW. Multi-objective optimization of tool path considering efficiency, energy-saving and carbon-emission for free-form surface milling. J Clean Prod 2018;172:3311–22. http://dx.doi.org/10.1016/j.jclepro.2017.07.219, URL https://www.sciencedirect.com/science/article/pii/S0959652617316748.

[27] Xu K, Li Y, Xiang B. Image processing-based contour parallel tool path optimization for arbitrary pocket shape. Int J Adv Manuf Technol 2019;102(5):1091–105.

[28] Hatem N, Yusof Y, Kadir AZA, Latif K, Mohammed M. A novel integrating between tool path optimization using an ACO algorithm and interpreter for open architecture CNC system. Expert Syst Appl 2021;178:114988.

[29] Kumar M, Khatak P. Development of a discretization methodology for 2.5 D milling toolpath optimization using genetic algorithm. In: Advances in computing and intelligent systems. Springer; 2020, p. 93–104.

[30] Karuppanan BRC, Saravanan M. Optimized sequencing of CNC milling toolpath segments using metaheuristic algorithms. J Mech Sci Technol 2019;33(2):791–800.

[31] Edem IF, Mativenga PT. Modelling of energy demand from computer numerical control (CNC) toolpaths. J Clean Prod 2017;157:310–21.
[32] Pezer D. Efficiency of tool path optimization using genetic algorithm in relation to the optimization achieved with the CAM software. Procedia Eng 2016;149:374–9.
[33] Chen T, Li M. The weights can be harmful: Pareto search versus weighted search in multi-objective search-based software engineering. ACM Trans Softw Eng Methodol 2022.
[34] Ishibuchi H, Doi K, Nojima Y. On the effect of normalization in MOEA/D for multi-objective and many-objective optimization. Complex Intell Syst 2017;3(4):279–94.
[35] Verma S, Pant M, Snasel V. A comprehensive review on NSGA-II for multi-objective combinatorial optimization problems. IEEE Access 2021;9:57757–91.
[36] Deb K, Pratap A, Agarwal S, Meyarivan T. A fast and elitist multiobjective genetic algorithm: NSGA-II. IEEE Trans Evol Comput 2002;6(2):182–97.
[37] Hu L, Tang R, Liu Y, Cao Y, Tiwari A. Optimising the machining time, deviation and energy consumption through a multi-objective feature sequencing approach. Energy Convers Manage 2018;160:126–40. http://dx.doi.org/10.1016/j.enconman.2018.01.005, URL https://www.sciencedirect.com/science/article/pii/S0196890418300050.
[38] Xue Y. Mobile robot path planning with a non-dominated sorting genetic algorithm. Appl Sci 2018;8(11):2253.
[39] Beirigo BA, dos Santos AG. Application of NSGA-II framework to the travel planning problem using real-world travel data. In: 2016 IEEE congress on evolutionary computation. IEEE; 2016, p. 746–53.
[40] Alpers B. On fast jerk–, acceleration–and velocity–restricted motion functions for online trajectory generation. Robotics 2021;10(1):25.
[41] Tajima S, Sencer B. Global tool-path smoothing for CNC machine tools with uninterrupted acceleration. Int J Mach Tools Manuf 2017;121:81–95. http://dx.doi.org/10.1016/j.ijmachtools.2017.03.002, Special Issue on the State-of-the-Art in North American Manufacturing Research, URL https://www.sciencedirect.com/science/article/pii/S089069551630493X.
[42] Hassanat AB, Prasath V, Abbadi MA, Abu-Qdari SA, Faris H. An improved genetic algorithm with a new initialization mechanism based on regression techniques. Information 2018;9(7):167.
[43] Li C, Zhu Z, Yang H, Li R. An innovative hybrid system for wind speed forecasting based on fuzzy preprocessing scheme and multi-objective optimization. Energy 2019;174:1219–37.
[44] Tian Y, Wang H, Zhang X, Jin Y. Effectiveness and efficiency of non-dominated sorting for evolutionary multi-and many-objective optimization. Complex Intell Syst 2017;3(4):247–63.